An internal GAP domain negatively regulates presynaptic dynamin in vivo: a two-step model for dynamin function

Radhakrishnan Narayanan,[1] Marilyn Leonard,[2] Byeong Doo Song,[2] Sandra L. Schmid,[2] and Mani Ramaswami[1]

[1]Department of Molecular and Cellular Biology and Arizona Research Laboratories Division of Neurobiology, University of Arizona, Tucson, AZ 85721
[2]Department of Cell Biology, The Scripps Research Institute, La Jolla, CA 92037

The mechanism by which the self-assembling GTPase dynamin functions in vesicle formation remains controversial. Point mutations in *shibire*, the *Drosophila* dynamin, cause temperature-sensitive (ts) defects in endocytosis. We show that the ts2 mutation, which occurs in the switch 2 region of dynamin's GTPase domain, compromises GTP binding affinity. Three second-site suppressor mutations, one in the switch 1 region of the GTPase domain and two in the GTPase effector domain (GED), dynamin's putative GAP, fully rescue the shi^{ts2} defects in synaptic vesicle recycling. The functional rescue in vivo correlates with a reduction in both the basal and assembly-stimulated GTPase activity in vitro. These findings demonstrate that GED is indeed an internal dynamin GAP and establish that, as for other GTPase superfamily members, dynamin's function in vivo is negatively regulated by its GAP activity. Based on these and other observations, we propose a two-step model for dynamin during vesicle formation in which an early regulatory GTPase-like function precedes late, assembly-dependent steps during which GTP hydrolysis is required for vesicle release.

Introduction

Several important insights into dynamin's function in vesicle formation have been revealed by genetic analyses of *Drosophila shibire*^{ts} (shi^{ts}) mutants that have temperature-sensitive (ts) defects in dynamin function (Poodry et al., 1973; Kosaka and Ikeda, 1983; Chen et al., 1991; van der Bliek and Meyerowitz, 1991; Grant et al., 1998). At nonpermissive temperatures, shi^{ts} mutants show rapid paralysis due to use-dependent depletion of synaptic vesicles (Poodry and Edgar, 1979). Concurrently, the formation of endocytic vesicles from the presynaptic membrane is arrested at a stage where a protein "collar" surrounds the necks of endocytic intermediates trapped before membrane fission (Kosaka and Ikeda, 1983). Consistent with the semi-dominant phenotypes of shi^{ts} mutants, purified dynamin forms an oligomeric unit that further assembles into helical structures remarkably similar to collars observed on shi^{ts1} presynaptic membranes (Kim and Wu, 1990; Hinshaw and Schmid, 1995; Takei et al., 1995; Sweitzer and Hinshaw, 1998). Dynamin is an atypical GTPase in that it has a low affinity for GTP, a very high rate of GDP dissociation (Binns et al., 1999), and a relatively high intrinsic rate of GTP hydrolysis, which is further stimulated by self-assembly (Song et al., 2004b). Dynamin is the major GTPase associated with membrane internalization and its abilities to bind and hydrolyze GTP, together with GTP-driven conformational changes, are required for endocytic vesicle formation (Marks et al., 2001; Song and Schmid, 2003).

Despite intense study, the exact function of GTP hydrolysis by dynamin in vivo and mechanisms of its regulation remain controversial. Dynamin assembly onto artificial templates stimulates GTP hydrolysis by 50- to 100-fold, and it has been proposed that the GTPase effector domain (GED) of dynamin functions as an intramolecular, assembly-dependent GAP (Muhlberg et al., 1997; Sever et al., 1999). However, recent observations have brought this into question, leading to the alternate proposal that GED functions solely as an assembly domain, and not a GAP (Marks et al., 2001). Moreover, the function of assembly-stimulated GTP hydrolysis by dynamin is particularly controversial. In one view, dynamin's assembly-dependent GAP activity acts as a negative regulator of dynamin function (Sever et al., 1999, 2000). In the alternative view, the rapid assembly-stimulated GTP hydrolysis drives a concerted conformational change, akin to a "powerstroke," that generates the force

Correspondence to Mani Ramaswami: mani@u.arizona.edu; or Sandra L. Schmid: slschmid@scripps.edu

Abbreviations used in this paper: GED, GTPase effector domain; LT, lipid tubule; shi^{ts}, $shibire^{ts}$; *Sushi*, suppressor of *shi*; ts, temperature sensitive; wt, wild-type.

The online version of this article includes supplemental material.

The Journal of Cell Biology, Vol. 169, No. 1, April 11, 2005 117–126
http://www.jcb.org/cgi/doi/10.1083/jcb.200502042

necessary for membrane fission (Hinshaw and Schmid, 1995; Sweitzer and Hinshaw, 1998; Marks et al., 2001).

These important issues have been difficult to resolve, in part because mutations that clearly separate different functions of dynamin have been hard to obtain. For instance, mutations that inhibit GED-stimulated GTP hydrolysis in vitro also inhibit dynamin assembly (Sever et al., 1999; Marks et al., 2001), and vice versa (Song et al., 2004b). Moreover, the cellular functions of these mutant proteins have been assessed after overexpression in wild-type (wt) cells. The presence of endogenous wt dynamin in these experiments may mask the effects of mutations, making them more moderate in amplitude, and/or otherwise complicate the interpretation of results. In this study, we have attempted to overcome these limitations by appropriate selection of *shibire* mutant alleles in *Drosophila*, analysis of their consequences on endocytosis in vivo, and characterization of their effects on biochemical activities of dynamin in vitro. Our findings provide new insight into the molecular mechanisms of dynamin function and its role in synaptic vesicle recycling.

Results

The *shi*^{ts2} mutation corresponds to a Gly to Ser substitution within the switch 2 region of the GTPase domain (Fig. 1 A), known to be involved in GTP binding and hydrolysis (van der Bliek and Meyerowitz, 1991). Our finding that *shi*^{ts2} mutant phenotypes are substantially aggravated by a reduction in nucleoside diphosphate kinase, an enzyme that provides GTP pools accessed by dynamin (Krishnan et al., 2001; Palacios et al., 2002), suggested that this mutation might compromise GTP binding. To test this hypothesis, we generated the ts2-homologous amino acid substitution (G146S) in human dynamin-1, whose biochemical properties in vitro have been thoroughly studied (for review see Song and Schmid, 2003). The validity of this experimental design is supported by (1) the high conservation of GTPase domain sequences (Fig. 1 A) between human and *Drosophila* dynamins (Chen et al., 1991; van der Bliek and Meyerowitz, 1991); (2) the fact that the entire three-dimensional structures of both GTPase domains are easily folded on a template crystal structure of the *Dictyostelium* dynamin A GTPase domain (Niemann et al., 2001) (Fig. 1 B); and (3) our finding that HeLa cells exhibit a ts defect in endocytosis similar to *shi*^{ts1} flies when overexpressing dyn1:G273D, the human homologue of *shi*^{ts1} (Damke et al., 1995).

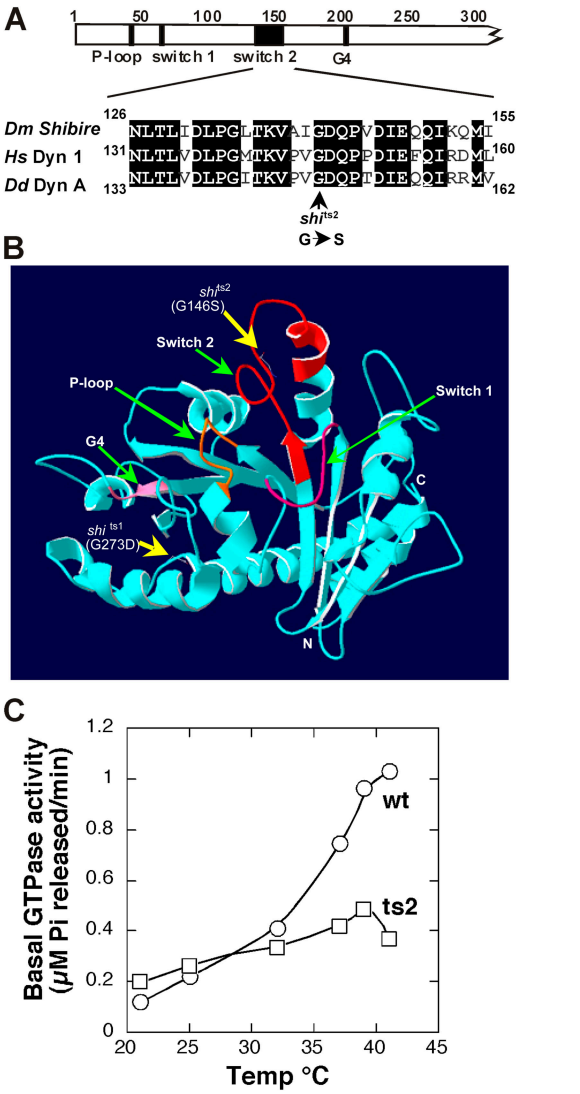

Figure 1. **The *shi*^{ts2} mutation (G146S) is in the highly conserved switch 2 region of the GTPase domain.** (A) Alignment of *Drosophila shibire*, human dynamin-1, and *Dictyostelium* dynamin A around the ts2 mutation shows tightly conserved residues. (B) Threaded structure of human dynamin-1 GTPase domain folded on a template crystal structure of *Dictyostelium* dynamin A GTPase domain (Niemann et al., 2001) using Geno3D automatic comparative modeling of three-dimensional protein structure (Combet et al., 2002) and Swiss-PdbViewer (http://www.expasy.org). The four consensus GTP binding elements (green arrows) and the locations of the ts1 and ts2 mutations (yellow arrows) are indicated. (C) Temperature dependence of basal GTPase activity of dyn1:wt (○) and dyn1:ts2 (□) measured in the presence of 100 μM GTP.

The *shi*^{ts2} mutation reduces GTP affinity

Wt and mutant dyn1:ts2 proteins were purified after expression using baculovirus vectors in insect cells and analyzed at various temperatures for GTPase activity (Fig. 1 C). As expected, the dyn1:ts2 mutant protein exhibited a pronounced ts defect in GTPase activity (Fig. 1 C), and the ts defect appeared to manifest itself at temperatures above 32°C. This in vitro temperature sensitivity profile corresponded exactly to that determined for defects in endocytosis in vivo when the *shi*^{ts1} mutation (G273D) was generated in human dynamin and expressed in HeLa cells (Damke et al., 1995), and likely reflects the fact that *shibire* and human dynamin have evolved to function at different temperatures. Consistent with this interpretation, when a point mutation in mammalian src kinase, which has a restrictive temperature of 37°C, was generated in the *Drosophila* Sevenless tyrosine kinase, the restrictive temperature shifted to 24°C (Simon et al., 1991). Based on these data, we chose room temperature (~20°C) as the permissive temperature and 39°C as the nonpermissive temperature.

To more precisely identify the ts biochemical defect of dyn1:ts2 responsible for the defect in endocytosis, we compared the Michaelis-Menten kinetics for basal GTPase activity

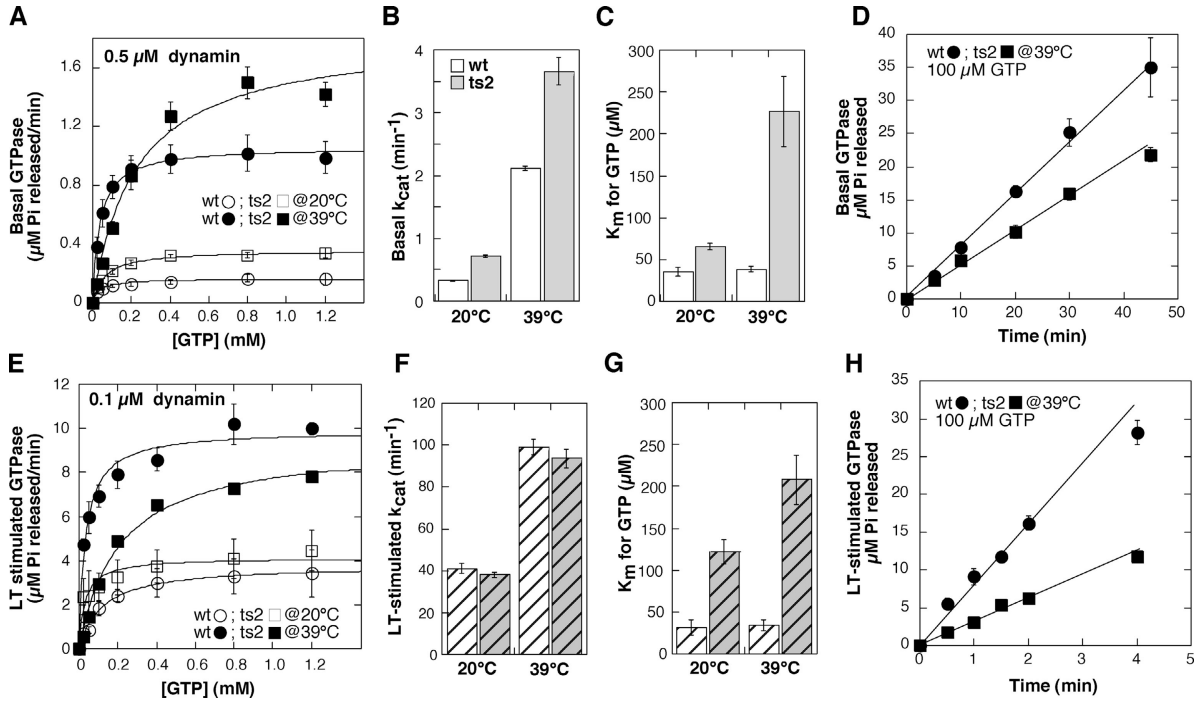

Figure 2. **Dyn1:ts2 has a ts defect in GTP binding.** (A) The basal rates of GTP hydrolysis were determined in the presence of varying concentrations of GTP for 0.5 μM dyn1:wt (○, ●) or dyn1:ts2 (□, ■) at 20 and 39°C, as described in Materials and methods. Shown are averaged data from three independent experiments ± SEM. The k_{cat} (B) and K_m (C) values for basal GTPase activity were calculated from the data in A. Errors are SDs from the best-fit curve to the data. (D) Time course of GTP hydrolysis at 39°C for dyn1:wt (●) and dyn1:ts2 (■) measured in the presence of physiological concentrations of GTP (100 μM). Shown are averaged data from three independent experiments ± SEM. (E–H) Same as for A–D, except that assembly-stimulated GTPase activity was measured in the presence of 0.1 mg/ml lipid nanotubules and 0.1 μM dynamin.

of wt and mutant dynamin at both 20 and 39°C (Fig. 2, A–C). In this analysis, k_{cat} measures the efficiency of GTP hydrolysis after binding, whereas K_m, the Michaelis-Menten constant, is a composite term reflecting the rate constants for GTP association, dissociation, and catalysis. Under basal GTPase assay conditions, when hydrolysis rates are low, K_m corresponds well with the affinity of dynamin for GTP (see Materials and methods). When unassembled dynamin was assayed at 20°C, both the k_{cat} and K_m were slightly increased for dyn1:ts2 relative to dyn1:wt (k_{cat} = 0.7 ± 0.01 min^{-1} and 0.3 ± 0.01 min^{-1}; and K_m = 65.7 ± 3.8 μM and 35.1 ± 5.3 μM, respectively, for dyn1:ts2 and dyn1:wt) (Fig. 2, B and C). The basal GTPase activities of both wt and dyn1:ts2 increased by approximately fivefold when assayed at 39°C, and the GTPase activity of dyn1:ts2 remained approximately twofold greater than wt (k_{cat} of 3.7 ± 0.2 min^{-1} vs. 2.1 ± 0.04 min^{-1}, respectively). The most significant temperature-dependent effect observed, however, was that the K_m for dyn1:ts2 assayed at 39°C was approximately sixfold increased compared with dyn1:wt (226 ± 42 μM vs. 38 ± 3 μM, respectively), suggesting a defect in GTP binding. This was confirmed using a filter assay to directly measure binding of [^{35}S]GTPγS to dynamin (see Fig. 5 G). From these results we conclude, as predicted from earlier genetic analysis, that dyn1:ts2 exhibits a ts defect in GTP binding.

Results consistent with this conclusion were also obtained when dynamin's assembly-stimulated GTP hydrolysis was measured using lipid tubules (LTs) as a template for dynamin self-assembly (Fig. 2, E–G). The GTPase activity of both proteins was increased 50- to 100-fold upon assembly onto LT templates, and the maximum rate of LT-stimulated GTPase activity measured at 39°C was similar for dyn1:ts2 (93.6 ± 4.4 min^{-1}) and dyn1:wt (99.1 ± 3.5 min^{-1}) (Fig. 2 F). In contrast, dyn1:ts2 exhibited an approximately sixfold increase in K_m for GTP compared with dyn1:wt (208 ± 29 vs. 34 ± 6, respectively) (Fig. 2 G). As the k_{cat} values for these two proteins are comparable, this suggests that dyn1:ts2 exhibits a sixfold decrease in binding affinity relative to dyn1:wt. Importantly, the proteins were found to be indistinguishable in their ability to self-assemble into sedimentable structures at low salt concentration (Fig. 3 A), or into sedimentable helical arrays on LTs at physiological salt concentration (Fig. 3, B and C). From these data we conclude that the major ts defect of dyn1:ts2 is its reduced ability to bind GTP.

To assess the likely consequences of this defect on the in vivo function of dynamin, we examined basal and LT-stimulated rates of GTP hydrolysis at 39°C in the presence of 100 μM GTP, its estimated concentration in cytosol (Otero, 1990). In the presence of this more physiologically relevant GTP concentration, the basal GTPase activity of the ts2 mutation is reduced to 60% of wt dynamin rates (Fig. 2 D), whereas the LT-stimulated GTPase activity showed a more pronounced defect and was reduced to 33% of wt dynamin rates (Fig. 2 H). Thus, the ts defect in endocytosis of *shi^{ts2}* mutant flies may derive either from the defect in GTP binding or from the consequent decrease in assembly-stimulated GTPase activity.

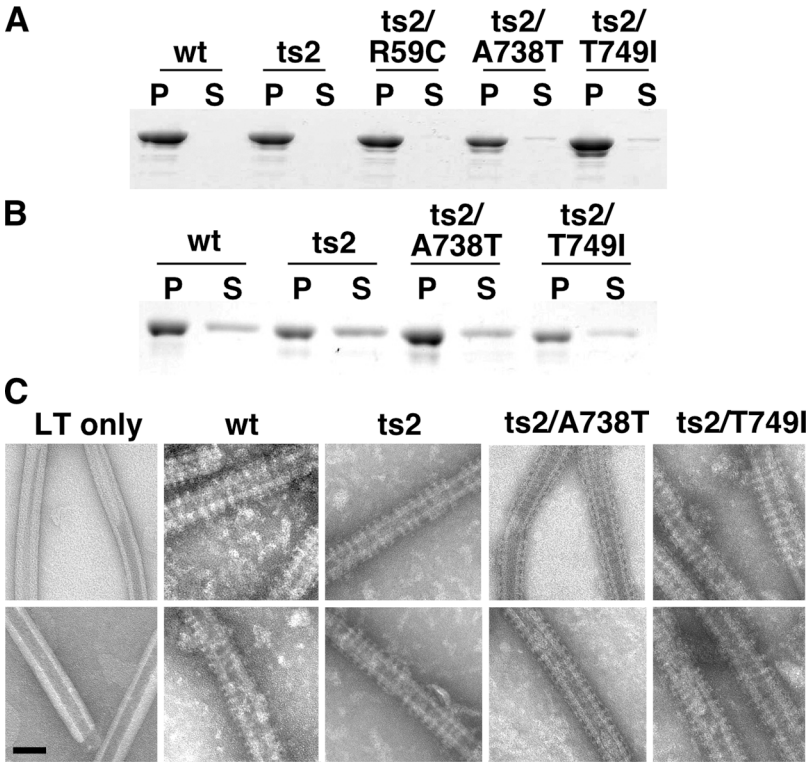

Figure 3. **Dyn1:ts2 and the *Sushi* mutants exhibit wt self-assembly activities.** (A) Wt and mutant dynamin proteins (2 μM) were incubated in 20 mM Hepes, pH 7.5, 2 mM $MgCl_2$, and 10 mM KCl for 20 min at 39°C. Mixtures were sedimented at 14,000 rpm for 10 min at 4°C; pellets (P) and supernatants (S) were collected and subjected to SDS-PAGE. Proteins were detected by Coomassie blue staining. (B) Wt and mutant dynamin proteins were incubated as above except in buffer containing 150 mM KCl and with LTs. Pellets and supernatants after sedimentation are shown. (C) Negative-stained electron micrographs of wt and mutant dynamins assembled onto PI-4,5-P_2–containing LTs. Bar, 50 nm.

Second-site mutations in switch 1 or GED suppress all *shi*^{ts2} phenotypes

Strong evidence that the defect in endocytosis in *shi*^{ts2} is due directly to its GTP binding defect rather than indirectly to a defect in GTP hydrolysis is derived from our analysis of a new class of dynamin mutants. The so-called Suppressor of shi (*Sushi*) mutations were identified in an earlier genetic screen for mutations that suppressed defects in *shi*^{ts2} dynamin (Ramaswami et al., 1993). These mutations did not perceptibly alter protein levels (Fig. 4 A, top), but dramatically rescued the ts, paralytic phenotype (Fig. 4 A, bottom). Similarly, synaptic transmission in the visual system of *Drosophila*, lost in *shi*^{ts2} mutants at 30°C, was restored by the suppressor mutations (Fig. S1, available at http://www.jcb.org/cgi/content/full/jcb.200502042/DC1). Multiple lines of experimentation establish that all of the synaptic defects in *shi*^{ts2} mutants were rescued by the *Sushi* mutations. Specifically, synaptic vesicle endocytosis, which can be directly monitored as uptake of the fluorescent tracer FM1-43 into stimulated nerve terminals (Betz and Bewick, 1992; Ramaswami et al., 1994), was completely blocked in *shi*^{ts2}, but occurred efficiently in the presence of the *Sushi* mutations (Fig. 4 B). The synaptic vesicle protein synaptotagmin, normally present in tight vesicle clusters localized within presynaptic varicosities, was redistributed along the axon of *shi*^{ts2} mutants stimulated at elevated temperatures (Estes et al., 1996); however, consistent with restored endocytosis, no such redistribution was observed in the presence of the suppressor mutations (Fig. 4 C). Finally, electrophysiological studies demonstrated that the synaptic depression that accompanies use-dependent vesicle depletion at *shi*^{ts2} nerve terminals was not observed in the presence of the suppressor mutations (Fig. 4 D). Thus, each of the suppressor mutations fully restores to wt both the behavioral and cellular defects of *shi*^{ts2} mutants.

Recombination analysis had mapped these *Sushi* alleles to within ~100 kb of the *shi* gene, identifying them as probable intragenic suppressors of *shi*^{ts2} (Ramaswami et al., 1993). The ts2 mutation is located within the switch 2 region of the GTPase domain, which in other GTPases undergoes major conformational changes in response to GTP binding and provides a site of interaction with GAP molecules (Vetter and Wittinghofer, 2001). Because the identity and biochemical effects of these mutations had the potential to establish specific mechanisms that underlie dynamin function, we sequenced the *shibire* gene in the *Sushi* mutant strains and confirmed that they were truly intragenic suppressors of *shi*^{ts2} (Fig. 4 E). One of the *Sushi* mutations (R59C, corresponding to *VS2*) mapped near the switch 1 region of dynamin's GTPase domain, which like switch 2 undergoes large conformational changes upon GTP binding and hydrolysis. Remarkably, two of the suppressor mutations (A738T and T749I, corresponding to *KVS* and *Shy*, respectively) mapped to the COOH-terminal region of GED, the putative assembly-dependent GAP domain of dynamin. These genetic data, in themselves, provide strong support for functional interactions between the switch 2/switch 1 and switch 2/GED regions of dynamin.

Sushi mutations reduce assembly-stimulated GTP hydrolysis

To explore the mechanisms by which *Sushi* mutations cause the observed dramatic functional suppression of *shi*^{ts2}, we expressed human dynamin corresponding to the three *Sushi* alleles

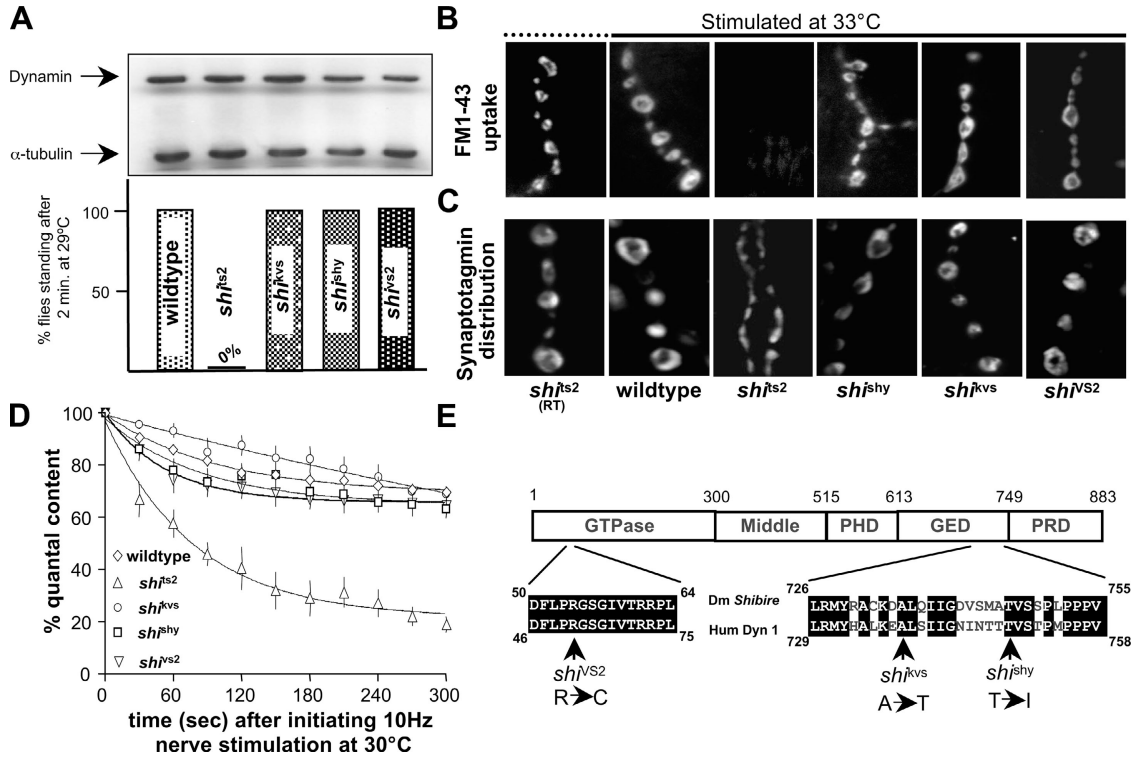

Figure 4. ***Sushi* mutations completely suppress *shi*^{ts2} mutant phenotypes.** (A) The three *Sushi* (suppressor of *shi*^{ts2}) mutations (*VS2*, *KVS*, and *Shy*) do not alter levels of dynamin (top), but all completely rescue the ts paralytic behavior of *shi*^{ts2} mutants (bottom). (B) Synaptic vesicle endocytosis, indicated by uptake of the fluorescent endocytic tracer FM1-43 into stimulated nerve terminals, is completely blocked in *shi*^{ts2} but occurs efficiently in the presence of the *Sushi* mutations. (C) The synaptic vesicle protein synaptotagmin is trapped on the presynaptic plasma membrane and diffuses along the axon of *shi*^{ts2} nerve terminals stimulated at elevated temperatures (third panel), but shows normal (left two panels) synaptic vesicle distribution in the presence of the *Shy*, *KVS*, or *VS2* mutations (right panels). (D) In the presence of the suppressor mutations, enhanced synaptic depression caused by use-dependent depletion of synaptic vesicles at *shi*^{ts2} nerve terminals stimulated at 10 Hz at 30°C is not observed ($n = 5$ for *ts2* and *VS2* and 4 for *Shy* and *KVS*). (E) Domain structure of dynamin including GTPase and GED, to which *Sushi* mutations *VS2*, *KVS*, and *Shy* are mapped. All three mutations identify residues conserved between *Drosophila shibire* and human dynamin-1.

(dyn1:ts2/T749I^{Shy}, dyn1:ts2/A738T^{KVS}, and dyn1:ts2/R59C^{VS2}) and analyzed their biochemical activities at 39°C, relative to the parent molecule, dyn1:ts2 (Fig. 5, A–F). Strikingly, none of the *Sushi* mutations repaired the ts2 defect in GTP binding as assessed, either by the K_m for GTP hydrolysis measured under basal conditions (Fig. 5 C) or directly using a filter-binding assay (Fig. 5 G). Although the K_m values for GTP hydrolysis measured under assembly conditions were significantly decreased in the *Sushi* mutants compared with dyn1:ts2 mutant (Fig. 5 F), they remained significantly higher than dyn1:wt. Moreover, as previously discussed, because LT-stimulated rates of GTP hydrolysis are high and variable for these different proteins, K_m measured under these conditions is not a direct measure of GTP binding affinity. Therefore, from these data we conclude that rescue of the endocytosis defect in vivo by the second-site *Sushi* mutants does not correlate with an increased GTP binding affinity measured in vitro.

Rather than reversing the GTP binding defect, each of the *Sushi* mutations instead resulted in a significant decrease in the basal GTPase activity relative to the parent molecule, dyn1:ts2 (Fig. 5 B). In the case of dyn1:ts2/A738T^{KVS} and dyn1:ts2/R59C^{VS2} the basal rates of GTP hydrolysis were threefold reduced relative to dyn1:ts2; whereas the basal rate of dyn1:ts2/T749I^{Shy} was twofold reduced relative to dyn1:ts2. Thus, in vivo rescue by all three second-site *Sushi* mutations correlated with a decrease in the basal GTPase activity of dyn:ts2.

The effects of the dyn1:ts2/T749I^{Shy} and dyn1:ts2/R59C^{VS2} mutations on assembly-stimulated GTPase activity were less pronounced, although both exhibited lower rates than either dyn1:wt or dyn1:ts2. Interestingly, the assembly-stimulated GTPase activity of dyn1:ts2/A738T^{KVS} was reduced by ~60% compared with either dyn1:ts2 or wt dynamin (Fig. 5 E), suggesting that assembly-stimulated GTPase activity may not be rate-limiting for dynamin function at the synapse. From these data we conclude that the reduced GTP hydrolysis rate of the parent *shi*^{ts2} protein observed at physiological GTP concentrations (Fig. 2, D and H) was not responsible for the endocytosis defect in vivo. Indeed, the ability of the second-site *Sushi* mutations to rescue the endocytosis defect in vivo correlated with their affecting a further reduction in the basal GTPase activity measured in vitro.

Mutations in the NH_2-terminal region of GED (e.g., K694A and I690K) were previously shown to inhibit dynamin self-assembly and thus to indirectly impair assembly-stimulated GTPase activity (Sever et al., 1999; Marks et al., 2001; Song et al., 2004b). In contrast, the *Sushi* mutations map to the COOH-terminal region of GED and have no effect on dynamin's ability to self-assemble, as assessed by sedimentation

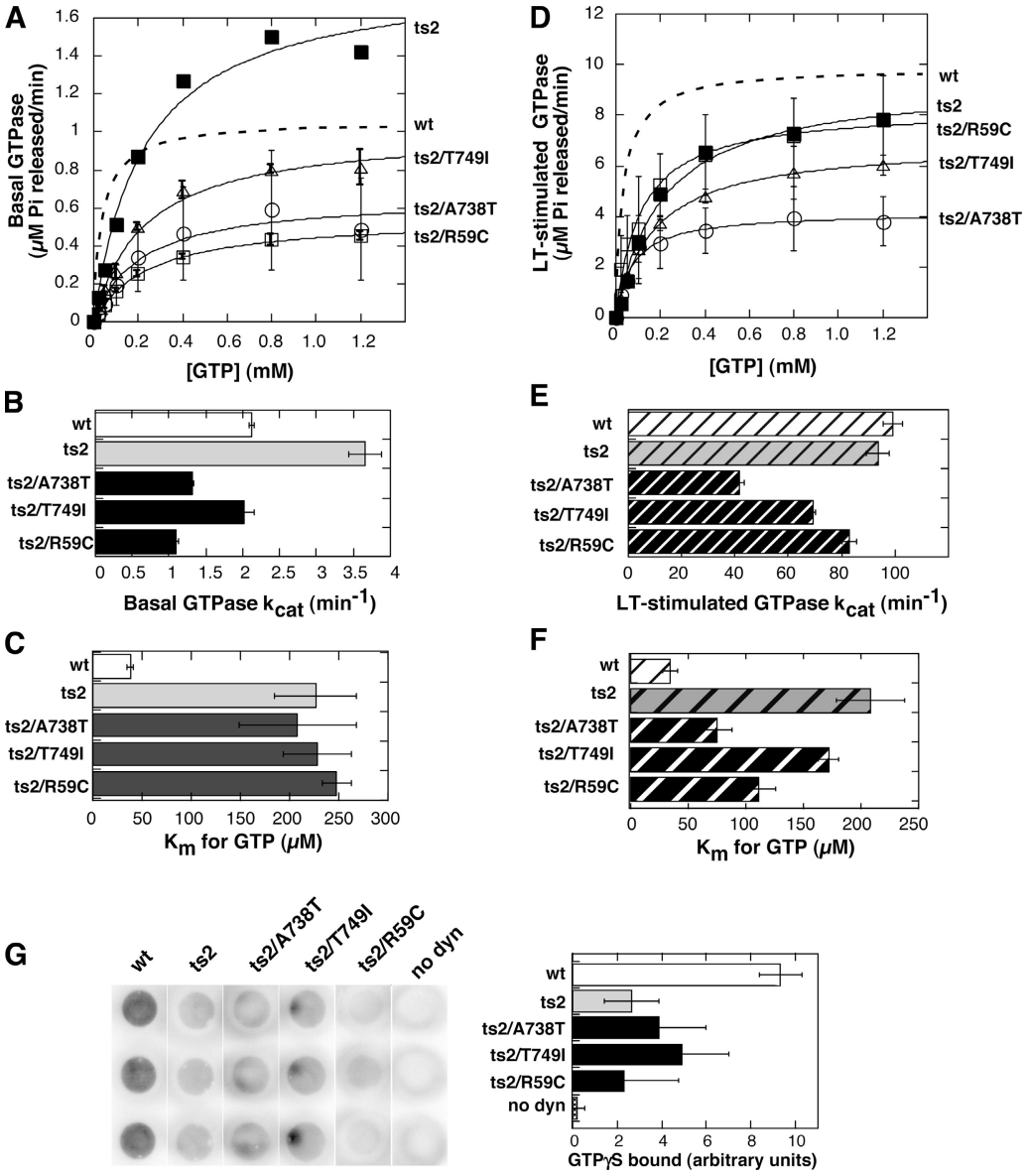

Figure 5. **Second-site *Sushi* mutations alter basal and assembly-stimulated rates of GTP hydrolysis.** (A) Unstimulated rates of GTP hydrolysis were determined at 39°C as described in Fig. 2 for dyn1:ts2/A738T^{KVS}, dyn1:ts2/T749I^{Shy}, and dyn1:ts2/R59C^{VS2} as indicated. Data for wt and ts2 are redrawn from Fig. 2. Values shown are averages from independent experiments ± SEM, $n = 3$ for dyn1:ts2/T749I^{Shy} and dyn1:ts2/R59C^{VS2}, $n = 6$ for dyn1:ts2/A738T^{KVS} because this mutant exhibited more variable results probably due to some aggregation, which would artificially enhance basal GTPase activity. The k_{cat} (B) and K_m (C) values for basal GTPase activity were calculated from the data in A. Errors are SDs from the best-fit curve to the data. (D–F) Same is in A–C except that the LT-stimulated rates of GTP hydrolysis were determined for each of the *Sushi* mutants in three independent experiments. (G) Filter assay for binding of [^{35}S]GTPγS to wt and mutant dynamins at 39°C, performed as described in Materials and methods. Shown are dot blots from a single experiment performed in triplicate, with or without 2 μM dynamin and 25 μM GTPγ^{35}S along with quantitation of the average ± SD from three such independent experiments.

assays either upon dilution into low salt buffers or when incubated with LTs at physiological salt (Fig. 3, A and B, respectively). The helical arrays formed by the *Sushi* GED mutants when assembled on LTs were indistinguishable by negative-stain EM from those observed with either dyn1:wt or dyn1:ts2 (Fig. 3 C). Moreover, although the absolute rates of assembly-stimulated GTPase activity for dyn1:ts2/T749I^{Shy} and dyn1:ts2/A738T^{KVS} were reduced relative to dyn1:ts2, all three proteins exhibited a comparable (~30-fold) increase in GTPase activity when assayed in the presence of the lipid template. Finally, because the *Sushi* mutants are fully functional in vivo and self-assembly is essential for endocytosis (Song et al., 2004b), it is unlikely that self-assembly is impaired by the COOH-terminally located *Sushi* mutations in GED.

We verified a role for the COOH-terminal residue A738 in assembly-stimulated GTPase activity by analyzing the biochemical properties of the single mutant, dyn1:A738T (Fig. S2, available at http://www.jcb.org/cgi/content/full/jcb.200502042/DC1). As expected, this single mutation in GED did not affect K_m, and interestingly had no effect on basal GTPase activity when expressed in the context of the wt GTPase domain. However, dyn1:A738T exhibited an ~50% reduction in LT-

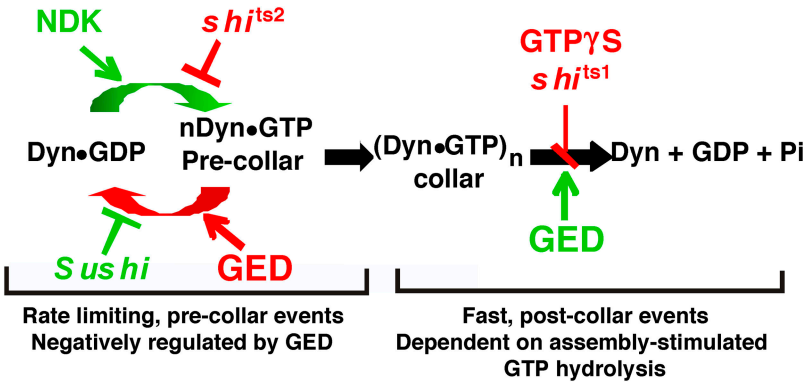

Figure 6. **Distinct early and late functions for dynamin: a two-step model for dynamin function in endocytosis.** A model that incorporates current and previously published observations (Kosaka and Ikeda, 1983; Hinshaw and Schmid, 1995; Takei et al., 1995; Sweitzer and Hinshaw, 1998; Sever et al., 1999; Marks et al., 2001) on dynamin's role in endocytosis. The model postulates an initial regulatory GTPase function for dynamin during a rate-determining precollar step in which the steady-state levels of dynamin GTP hydrolysis and/or dynamin•GTP are critical. These parameters are positively regulated by nucleoside diphosphate kinase (NDK) and negatively regulated by dynamin's GED, an internal GAP domain. The *shi*^{ts2} mutation impairs GTP binding, and the defect is restored by the three intragenic *Sushi* mutations, which impair GTPase activity and may function to stabilize dynamin•GTP. A subsequent post-collar step in endocytosis requires dynamin self-assembly and GTP hydrolysis, both of which are mediated, in part, by GED.

stimulated GTPase activity, similar to its effect on assembly-stimulated GTPase activity when present in the context of dyn1:ts2. Together, these data suggest that the novel *Sushi* mutations uncouple GED's role in self-assembly from GED's activity as an assembly-dependent GAP. Moreover, because a reduction in GED's GAP activity restores endocytosis, we conclude that GED negatively regulates dynamin's function in vivo.

Discussion

Intragenic suppressor analysis is a powerful tool to identify individual contributions of distinct biochemical activities contained in a complex enzyme (Shin et al., 2002). By characterizing biochemical defects in *shi*^{ts2} mutant dynamin and specifying activities altered by intragenic suppressor mutations isolated in a classical genetic screen, we are able to draw model-independent conclusions regarding mechanisms critical for function of the dynamin GTPase in synaptic vesicle recycling. Our results reveal that, as for classical GTPases, the switch 2 region in dynamin's GTPase domain participates in GTP binding and functionally interacts with GED, dynamin's GAP domain, to mediate both assembly-stimulated and basal GTPase activity. We identify residues in the COOH-terminal segment of GED that functionally interact with switch 2 and participate in its activity as a GAP domain mediating dynamin's assembly-stimulated GTP hydrolysis. Furthermore, the observed effects of the COOH-terminal GED mutations on basal GTPase activity suggest that GED might also function to stabilize the switch 2 region and contribute to catalysis in the unassembled state. This mechanism for stimulated GTPase activity is likely to be conserved among dynamin-related proteins, based on the observation that deletion of the last six amino acids in the functionally related COOH-terminal GED region of MxA abrogates its GTPase activity (Schwemmle et al., 1995). The data are consistent with a mechanism in which GED functions, like RGS-type GAPs (Scheffzek et al., 1998; Ross and Wilke, 2000), to regulate GTP hydrolysis by interacting with and stabilizing the switch 2 region of the GTPase domain.

The *Sushi* mutations were selected for their ability to restore the biological function of the ts2 mutant *shibire,* which we have shown is defective in GTP binding. Strikingly, restoration of *shi*^{ts2} function in vivo correlated not with an improved affinity for GTP—mutations rarely enhance protein function—but with a decrease in GTPase activity in vitro. The correlation was highest when we considered the GTPase activity of dynamin in its unassembled state. Our experiments show clearly that a mutant dynamin's compromised ability to bind GTP can be counter-balanced by a second-site mutation that compromises dynamin's GAP activity, suggesting that GAP activity functions, at least in part, to control the level of dynamin•GTP, and that this balance is essential for endocytosis in vivo. Thus, the simplest interpretation of our findings is that dynamin's GAP activity negatively regulates critical aspects of its function in vivo. This interpretation is consistent with the properties of all known GTPases. These findings are also consistent with earlier analyses of GED mutations (Sever et al., 2000), but make a far more compelling case, in part because these *Sushi* mutations in GED cleanly separate its function in assembly from its subsequent role in GTPase stimulation, and in part because the mutant dynamin replaces endogenous dynamin resulting in a far more dramatic in vivo phenotype.

Several laboratories have shown that dynamin's basal GTPase activity is essential for clathrin-mediated endocytosis (Herskovits et al., 1993; van der Bliek et al., 1993; Damke et al., 1994; Marks et al., 2001; Song et al., 2004a); thus, it is not surprising that the functional *Sushi* alleles still retain significant GTPase activity. That a two- to threefold decrease in GTPase activity of the dyn1:ts2 mutant in vitro suffices to restore *shi*^{ts2} function in vivo would be consistent with a critical role for dynamin GTPase activity as a kinetic timer monitoring endocytic events. Indeed, haplo-insufficiency of the dynamin-related protein OPA1 is known to cause inherited optic neuropathy in humans (Toomes et al., 2001), consistent with our suggestion that dynamin activity must be tightly regulated for correct in vivo function.

Arguments regarding the mechanisms governing dynamin's function in membrane fission have been polarized between purportedly exclusive models. However, the existence of a regulatory GTPase-like mechanism for unassembled dynamin during critical early stages of endocytosis does not exclude a subsequent requirement for self-assembly and assembly-stimulated GTP hydrolysis in late stages of endocytosis, as argued by several mutational and pharmacological studies

(Takei et al., 1995; Sever et al., 2000; Marks et al., 2001; Song and Schmid, 2003; Song et al., 2004b). Indeed, a function for dynamin after collar assembly has long been indicated by classic morphological studies of *shi*^{ts1} (Kosaka and Ikeda, 1983). Biochemical analyses of the GTPase properties of dyn1:ts1 (corresponding to G273D in human dynamin-1) were precluded by its complete inactivity in vitro (unpublished data). Nonetheless, that this post-collar function of dynamin occurs after GTP binding is indicated by the observation that, unlike *shi*^{ts2}, paralysis of *shi*^{ts1} flies is insensitive to reduction in levels of nucleoside diphosphate kinase (Chen et al., 2002).

Based on these considerations and our new findings, we suggest a two-step model for dynamin function (Fig. 6) in which an initial regulatory GTPase-like mechanism operates during early, rate-limiting steps in endocytosis, whereas self-assembly and assembly-stimulated GTP hydrolysis are essential for later stages in vesicle formation. In this model, dynamin might function early in endocytosis as a scaffolding molecule, interacting through its COOH-terminal proline/arginine-rich domain with SH3 domain–containing endocytic accessory factors that control coated pit assembly and maturation. It is possible that dynamin's interactions with SH3 domain–containing effectors are influenced by its GTP-bound state and/or by GTP turnover at steady state, although this has not been shown. Nonetheless, we suggest that dynamin's interactions with these effector molecules enables it to function as a kinetic timer monitoring molecular events during early stages of coated pit formation and maturation. At later stages, dynamin self-assembles at the necks where assembly-stimulated GTP hydrolysis may function directly in membrane fission. In this model, dynamin assembly controls the transition to late events in vesicle formation, and may be triggered by accessory proteins, for example amphiphysin or SNX9 (Yoshida et al., 2004; Soulet et al., 2005) and/or by the accumulation of dynamin•GTP, as it is known that dynamin self-assembly, under physiological conditions, is strongly enhanced in the presence of nonhydrolyzable analogues of GTP (Takei et al., 1995; Carr and Hinshaw, 1997). Finally, there is now considerable evidence that GTP hydrolysis by assembled dynamin drives concerted conformational changes that can generate a constrictive force on liposomes and LTs, which would facilitate vesicle release. (Sweitzer and Hinshaw, 1998; Stowell et al., 1999; Takei et al., 1999; Marks et al., 2001; Danino et al., 2004) GTP hydrolysis also triggers rapid disassembly of the dynamin complex (Warnock et al., 1996), which might influence interactions with accessory proteins required for membrane fission and/or recycling. Although we provide compelling evidence that presynaptic dynamin functions mechanistically like a regulatory GTPase whose activity is negatively regulated by an internal GAP, further experiments are required to completely establish the details of both early and post-collar events in endocytic vesicle formation.

Materials and methods

Drosophila culture and stocks

Flies were raised on medium consisting of instant food, agar, and oatmeal supplemented with yeast. All stocks were maintained at 25°C under uncrowded conditions, except for *shi*^{ts} stocks, which were maintained at 21°C. Wt Oregon-R was from Danny Brower's lab (University of Arizona, Tucson, AZ); *shi* and *Sushi* mutant alleles were from the Ramaswami lab collection.

Sequencing *Sushi* mutations

Sequencing of *Sushi* mutations was performed after detecting mutations in *shi* coding sequences PCR amplified from heterozygous *Sushi* cDNA. Mutation detection was done using dHPLC that detects altered melting temperature of DNA duplexes with single-base mismatches. After mutation detection, specific polymorphic cDNA fragments were amplified and sequenced. Both mutation detection and sequencing were done in the Genomics and Technology Core (GATC) facility at the University of Arizona.

Western blotting

For Western blotting, samples were subjected to SDS-PAGE and gels were electroblotted onto Hybond-PVDF (Amersham Biosciences), blocked with 5% nonfat dry milk powder in PBS/0.5% Tween 20, and incubated with a 1:1,000 dilution of anti-dynamin Ab2074. A 1:1,000 dilution of mouse monoclonal anti-tubulin was used as loading control. Detection was done with an HRP-conjugated secondary antibody (Cappel) and developed with an ECL detection system (Amersham Biosciences), according to the manufacturer's directions. For comparing relative amounts of dynamin, we selected a dilution of lysate (1/2 head for dynamin) at which the ECL signal was maximally sensitive, and corresponded roughly linearly, to protein concentration.

Analysis of synaptic depression

Electrophysiological recordings were made from larval bodywall muscle 6 within A2, with the larval preparation immersed in a low volume of the HL3 saline. Electrophysiology was performed as described previously (Narayanan et al., 2000). Larvae were dissected and positioned on a sylgard dish tightly clamped on a custom-designed stage that could be heated and cooled with a Peltier temperature controller (Physitemp). At a bath temperature of 30°C, larval ventral longitudinal muscle 6 was impaled with a glass microelectrode. In all experiments, the central nervous system was gently removed to prevent endogenous motor firing. Motor nerves were stimulated with glass-tipped suction electrodes. For intracellular recordings, electrodes pulled from borosilicate capillary tubes were backfilled with 3 M KCl, yielding resistances of 10–15 MΩ. To ensure good recordings, preparations with resting potentials more positive than −60 mV were discarded. Excitatory junction potentials (EJPs) were elicited by stimuli delivered at 10 Hz and were recorded with Axoscope 1.0 software (Axon Instruments, Inc.). The combination of high temperature and high frequency stimulation occasionally led to nerve conduction failure in the larval preparation. To ensure continuous nerve activity, we increased the stimulus pulse duration to 5 ms and carefully monitored EJPs to verify recruitment of both motor neurons, adjusting the stimulus intensity as necessary. We determined EJP amplitude for each time point (taken at 30-s intervals) by taking the average of five EJPs measured at this time point. The data shown derive from 3–5 different larvae of each genotype. Quantal content for each time point was calculated using a correction factor to account for nonlinear summation of quanta (Martin, 1955). Data plotting was done based on the nonlinear regression curve-fitting method using GraphPad software.

Analysis of FM1-43 uptake at larval motor terminals

Wandering third-instar larvae were filleted to reveal the entire musculature and nervous system; the central nervous system was left attached. Because complete block in endocytosis at *shi*^{ts} larval motor terminals requires temperatures ~6°C higher than the restrictive temperature for adult paralysis (Ramaswami et al., 1994), we tested for endocytic block at 33°C. High K^+ stimulation was with 60 mM K^+ saline for 2 min at 33°C in the presence of 4 μM FM1-43. We initially focused our attention on the synapses innervating muscles 6 and 7 of abdominal segments A-2 and A-3; however, we observed more consistent results when we considered all of the visible muscle fibers. The preparations were examined with a Zeiss Axioskop through a water immersion lens (63×, NA 0.9). Images were captured using a chilled CCD camera (Princeton Instruments) and MetaMorph software (Universal Imaging Corp.). After background subtraction (muscle surface close to bright boutons), digitized images were identically stretched and processed to maximize contrast in the brighter image, while preserving the relative intensities between control and experimental samples. Experiments were performed in pairs—one control and one experimental animal were treated together.

Analysis of synaptotagmin distribution in boutons

High K^+ stimulation was with 60 mM K^+ saline for 5 min at the specified temperature. After stimulation and before fixation, the high K^+ saline was

replaced briefly (~5 s) with prewarmed calcium-free saline to relax the preparation. Fixation and synaptotagmin antibody staining were done as previously described (Narayanan et al., 2000) using anti-synaptotagmin pAb (DSYT-2) from Hugo Bellen and Texas red–conjugated anti–rabbit secondary antibodies (Cappel). Images of bouton fields in muscle 6 and 7 were obtained with a 100× objective, 1.3 NA oil-immersion objective using a cooled CCD camera (Princeton Instruments with a KAF1400 chip) and MetaMorph software (Universal Imaging Corp.). 30-μm-thick sections of the bouton fields were deconvolved using Autodeblur and single sections showing a single branch of boutons were selected.

Baculovirus-based expression of mutant dynamins

Point mutations corresponding to ts2 (G146S) with or without the second-site *Sushi* mutants, corresponding to VS2 (R59C), KVS (A738T), and Shy (T749I) were introduced into human dynamin 1 by the QuikChange method (Stratagene), following manufacturer's instructions. All constructs were confirmed by sequencing. Recombinant baculoviruses were generated using BaculoGold linearized baculovirus DNA according to the manufacturer's instructions (BD Biosciences). Dynamin was expressed in Tn5 insect cells and purified by affinity chromatography using amphiphysin II SH3 domain conjugated to GST (SH3-GST) (Marks et al., 2001). Purified dynamin was dialyzed against the storage buffer (20 mM Hepes, pH 7.5, 150 mM KCl, 1 mM EDTA, 1 mM EGTA, and 1 mM DTT) and stored at −80°C after freezing in liquid nitrogen. Protein concentration was determined by OD280 using the extinction coefficient of 56170 for dynamin. Results presented were verified with two independent preparations of wt and mutant dynamins.

Determining K_m and k_{cat} for basal and LT-stimulated GTPase activities

GTP hydrolysis was measured at various concentrations of GTP using a colorimetric assay to detect released inorganic phosphate, in the absence or presence of PI-4,5-P_2–containing lipid nanotubules, as previously described (Song et al., 2004b). The initial, linear rate of GTP hydrolysis at each concentration of GTP was determined from the time courses and plotted against the concentration of GTP. The data shown are average values ± SEM from three independent experiments generated using two independently purified preparations of each protein. The Michaelis-Menten rate constants were determined using KaleidaGraph software by curve-fitting the data to the Henri-Michaelis-Menten equation (Rate of GTP hydrolysis = Vmax[GTP]/K_m + [GTP]) for the reaction:

$$\text{dynamin} + \text{GTP} \underset{k_{off}}{\overset{k_{on}}{\rightleftharpoons}} \text{dynamin}\bullet\text{GTP} \xrightarrow{k_{cat}} \text{dynamin} + \text{GDP} + \text{Pi}$$

$K_m = (k_{off} + k_{cat})/k_{on}$, whereas $Kd = k_{off}/k_{on}$; therefore, under conditions of basal GTPase activity, the K_m for GTP closely approximates the Kd for GTP binding because the GTP off-rate of 2 s^{-1} (Binns et al., 1999) is high compared with the basal GTP hydrolysis rate of ~0.03–0.06 s^{-1}.

Filter assay for GTP binding

Direct binding of [^{35}S]GTPγS (40 μCi/ml, Amersham Biosciences) to dynamin was measured using a filter-binding assay (Maeda et al., 1992; Marks et al., 2001), modified as previously described (Song et al., 2004a) to give reproducible results despite dynamin's low affinity (>10 μM) and the very rapid dissociation rate constant (2 min^{-1}) for GTP (Binns et al., 1999). As controls we showed that binding was inhibited by unlabeled GTP, but not ATP, and confirmed that the dynamin mutants known to be defective in GTP binding indeed bind only background levels of nucleotide (Song et al., 2004a).

EM of dynamin assembled on lipid nanotubules

Wt and mutant dynamins (10 μM) were incubated with P-I4,5-P_2–containing LTs at 39°C and then were adsorbed to carbon-coated EM grids. Samples were negatively stained with 1% uranyl acetate, then viewed and photographed using an electron microscope (Philips) at 105,000×. Negatives were scanned, and then inverted and adjusted for contrast using Adobe Photoshop.

Online supplemental material

Fig. S1 shows representative electroretinograms of the light-evoked visual responses recorded in the eyes of wt, shi^{ts2}, and *Sushi* mutant flies. The data show that the ts synaptic transmission defect measured in shi^{ts2} flies is corrected by each of the three *Sushi* mutations. Fig. S2 shows the Michael-Menten kinetics for basal and LT-stimulated GTPase activities of two independently isolated preparations of dyn1:A738T compared with dyn1:wt. Assays were performed in triplicate. Online supplemental material available at http://www.jcb.org/cgi/content/full/jcb.200502042/DC1.

We acknowledge Steven Sholly for his initial contributions to these studies and K.S. Krishnan for sharing unpublished information, and for his long-standing collaboration with M. Ramaswami on the genetics of *shibire*. We thank K.S. Krishnan, Jean Wilson, and the Schmid lab for comments on the manuscript; Alisa Jones for help with protein expression and purification; S. Sanyal for assistance with electrophysiology; and Malcolm Wood for help with negative-stain EM.

This work was funded by National Institutes of Health grants NS34889 and NS02001 and a Science Foundation of Ireland Research Professorship (to M. Ramaswami), and GM42455, R37-MH61345 (to S.L. Schmid). This is The Scripps Research Institute manuscript No. 16340-CB.

Submitted: 7 February 2005
Accepted: 25 February 2005

References

Betz, W.J., and G.S. Bewick. 1992. Optical analysis of synaptic vesicle recycling at the frog neuromuscular junction. *Science.* 255:200–203.

Binns, D.D., B. Barylko, N. Grichine, A.L. Adkinson, M.K. Helms, D.M. Jameson, J.F. Eccleston, and J.P. Albanesi. 1999. Correlation between self-association modes and GTPase activation of dynamin. *J. Protein Chem.* 18:277–290.

Carr, J.F., and J.E. Hinshaw. 1997. Dynamin assembles into spirals under physiological salt conditions upon the addition of GDP and gamma-phosphate analogues. *J. Biol. Chem.* 272:28030–28035.

Chen, M.L., D. Green, L. Liu, Y.C. Lam, L. Mukai, S. Rao, S. Ramagiri, K.S. Krishnan, J.E. Engel, J.J. Lin, and C.F. Wu. 2002. Unique biochemical and behavioral alterations in *Drosophila shibire^{ts1}* mutants imply a conformational state affecting dynamin subcellular distribution and synaptic vesicle cycling. *J. Neurobiol.* 53:319–329.

Chen, M.S., R.A. Ober, C.C. Schroeder, T.W. Austin, C.A. Poodry, S.C. Wadsworth, and R.B. Vallee. 1991. Multiple forms of dynamin are encoded by *shibire*, a *Drosophila* gene involved in endocytosis. *Nature.* 351:583–586.

Combet, C., M. Jambon, G. Deleage, and C. Geourjon. 2002. Geno3D: automatic comparative molecular modelling of protein. *Bioinformatics.* 18:213–214.

Damke, H., T. Baba, D.E. Warnock, and S.L. Schmid. 1994. Induction of mutant dynamin specifically blocks endocytic coated vesicle formation. *J. Cell Biol.* 127:915–934.

Damke, H., T. Baba, A.M. van der Bliek, and S.L. Schmid. 1995. Clathrin-independent pinocytosis is induced in cells overexpressing a temperature-sensitive mutant of dynamin. *J. Cell Biol.* 131:69–80.

Danino, D., K.H. Moon, and J.E. Hinshaw. 2004. Rapid constriction of lipid bilayers by the mechanochemical enzyme dynamin. *J. Struct. Biol.* 147:259–267.

Estes, P.S., J. Roos, A. van der Bliek, R.B. Kelly, K.S. Krishnan, and M. Ramaswami. 1996. Traffic of dynamin within individual *Drosophila* synaptic boutons relative to compartment specific markers. *J. Neurosci.* 16:5443–5456.

Grant, D., S. Unadkat, A. Katzen, K.S. Krishnan, and M. Ramaswami. 1998. Probable mechanisms underlying interallelic complementation and temperature-sensitivity of mutations at the *shibire* locus of *Drosophila melanogaster*. *Genetics.* 149:1019–1030.

Herskovits, J.S., C.C. Burgess, R.A. Obar, and R.B. Vallee. 1993. Effects of mutant rat dynamin on endocytosis. *J. Cell Biol.* 122:565–578.

Hinshaw, J.E., and S.L. Schmid. 1995. Dynamin self assembles into rings suggesting a mechanism for coated vesicle budding. *Nature.* 374:190–192.

Kim, Y.T., and C.F. Wu. 1990. Allelic interactions at the *shibire* locus of *Drosophila*: effects on behavior. *J. Neurogenet.* 7:1–14.

Kosaka, T., and K. Ikeda. 1983. Possible temperature-dependent blockage of synaptic vesicle recycling induced by a single gene mutation in *Drosophila*. *J. Neurobiol.* 14:207–225.

Krishnan, K.S., R. Rikhy, S. Rao, M. Shivalkar, M. Mosko, R. Narayanan, P. Etter, P.S. Estes, and M. Ramaswami. 2001. Nucleoside diphosphate kinase, a source of GTP, is required for dynamin-dependent synaptic vesicle recycling. *Neuron.* 30:197–210.

Maeda, K., T. Nakata, Y. Noda, R. Sato-Yoshitake, and N. Hirokawa. 1992. Interaction of dynamin with microtubules: its structure and GTPase activity investigated by using highly purified dynamin. *Mol. Biol. Cell.* 3:1181–1194.

Marks, B., M.H.B. Stowell, Y. Vallis, I.G. Mills, A. Gibson, C.R. Hopkins, and

H.T. McMahon. 2001. GTPase activity of dynamin and resulting conformation change are essential for endocytosis. *Nature.* 410:231–235.

Martin, A.R. 1955. A further study of the statistical composition on the endplate potential. *J. Physiol.* 130:114–122.

Muhlberg, A.B., D.E. Warnock, and S.L. Schmid. 1997. Domain structure and intramolecular regulation of dynamin GTPase. *EMBO J.* 16:6676–6683.

Narayanan, R., H. Kramer, and M. Ramaswami. 2000. *Drosophila* endosomal proteins hook and deep orange regulate synapse size but not synaptic vesicle recycling. *J. Neurobiol.* 45:105–119.

Niemann, H.H., M.L. Knetsch, A. Scherer, D.J. Manstein, and F.J. Kull. 2001. Crystal structure of a dynamin GTPase domain in both nucleotide-free and GDP-bound forms. *EMBO J.* 20:5813–5821.

Otero, A.D. 1990. Transphosphorylation and G protein activation. *Biochem. Pharmacol.* 39:1399–1404.

Palacios, F., J.K. Schweitzer, R.L. Boshans, and C. D'Souza-Schorey. 2002. ARF6-GTP recruits Nm23-H1 to facilitate dynamin-mediated endocytosis during adherens junctions disassembly. *Nat. Cell Biol.* 4:929–936.

Poodry, C.A., and L. Edgar. 1979. Reversible alterations in the neuromuscular junction of *Drosophila melanogaster* bearing a temperature-sensitive mutation, *shibire. J. Cell Biol.* 81:520–527.

Poodry, C.A., L. Hall, and D.T. Suzuki. 1973. Developmental properties of *shibire*: a pleiotropic mutation affecting larval and adult locomotion and development. *Dev. Biol.* 32:373–386.

Ramaswami, M., S. Rao, A. van der Bliek, R.B. Kelly, and K.S. Krishnan. 1993. Genetic studies on dynamin function in *Drosophila*. *J. Neurogenet.* 9:73–87.

Ramaswami, M., K.S. Krishnan, and R.B. Kelly. 1994. Intermediates in synaptic vesicle recycling revealed by optical imaging of *Drosophila* neuromuscular junctions. *Neuron.* 13:363–375.

Ross, E.M., and T.M. Wilke. 2000. GTPase-activating proteins for heterotrimeric G-proteins: regulators of G protein signaling (RGS) and RGS-like proteins. *Annu. Rev. Biochem.* 69:795–827.

Scheffzek, K., R. Ahmadian, and A. Wittinghofer. 1998. GTPase-activating proteins: helping hands to complement active site. *Trends Biochem. Sci.* 23:257–262.

Schwemmle, M., M.F. Richter, C. Hermann, N. Nassar, and P. Staeheli. 1995. Unexpected structural requirements for GTPase activity of the interferon-induced MxA protein. *J. Biol. Chem.* 270:13518–13523.

Sever, S., A.B. Muhlberg, and S.L. Schmid. 1999. Impairment of dynamin's GAP domain stimulates receptor-mediated endocytosis. *Nature.* 398:481–486.

Sever, S., H. Damke, and S.L. Schmid. 2000. Dynamin:GTP controls the formation of constricted coated pits, the rate limiting step in clathrin-mediated endocytosis. *J. Cell Biol.* 150:1137–1148.

Shin, B.S., D. Maag, A. Roll-Mecak, M.S. Arefin, S.K. Burley, J.R. Lorsch, and T.E. Dever. 2002. Uncoupling of initiation factor eIF5B/IF2 GTPase and translational activities by mutations that lower ribosome affinity. *Cell.* 111:1015–1025.

Simon, M.A., D.D. Bowtell, G.S. Dodson, T.R. Laverty, and G.M. Rubin. 1991. Ras1 and a putative guanine nucleotide exchange factor perform crucial steps in signaling by the sevenless protein tyrosine kinase. *Cell.* 67:701–716.

Song, B.D., and S.L. Schmid. 2003. A molecular motor or a regulator? Dynamin's in a class of its own. *Biochemistry.* 42:1369–1376.

Song, B.D., M. Leonard, and S.L. Schmid. 2004a. Dynamin GTPase domain mutants that differentially affect GTP binding, GTP hydrolysis, and clathrin-mediated endocytosis. *J. Biol. Chem.* 279:40431–40436.

Song, B.D., D. Yarar, and S.L. Schmid. 2004b. An assembly-incompetent mutant establishes a requirement for dynamin self-assembly in clathrin-mediated endocytosis in vivo. *Mol. Biol. Cell.* 15:2243–2252.

Soulet, F., D. Yarar, M. Leonard, and S.L. Schmid. 2005. SNX9 regulates dynamin assembly and is required for efficient clathrin-mediated endocytosis. *Mol. Biol. Cell.* 16:2058–2067.

Stowell, M.H.B., B. Marks, P. Wigge, and H.T. McMahon. 1999. Nucleotide-dependent conformational changes in dynamin: evidence for a mechanochemical molecular spring. *Nat. Cell Biol.* 1:27–32.

Sweitzer, S., and J. Hinshaw. 1998. Dynamin undergoes a GTP-dependent conformational change causing vesiculation. *Cell.* 93:1021–1029.

Takei, K., P.S. McPherson, S.L. Schmid, and P. De Camilli. 1995. Tubular membrane invaginations coated by dynamin rings are induced by GTPγS in nerve terminals. *Nature.* 374:186–190.

Takei, K., V.I. Slepnev, V. Haucke, and P. De Camilli. 1999. Functional partnership between amphiphysin and dynamin in clathrin-mediated endocytosis. *Nat. Cell Biol.* 1:33–39.

Toomes, C., N.J. Marchbank, D.A. Mackey, J.E. Craig, R.A. Newbury-Ecob, C.P. Bennett, C.J. Vize, S.P. Desai, G.C. Black, N. Patel, et al. 2001. Spectrum, frequency and penetrance of OPA1 mutations in dominant optic atrophy. *Hum. Mol. Genet.* 10:1369–1378.

van der Bliek, A.M., and E.M. Meyerowitz. 1991. Dynamin like protein encoded by the *Drosophila shibire* gene associated with vesicular traffic. *Nature.* 351:411–414.

van der Bliek, A.M., T.E. Redelmeier, H. Damke, E.J. Tisdale, E.M. Meyerowitz, and S.L. Schmid. 1993. Mutations in human dynamin block an intermediate stage in coated vesicle formation. *J. Cell Biol.* 122:553–563.

Vetter, I.R., and A. Wittinghofer. 2001. The guanine nucleotide-binding switch in three dimensions. *Science.* 294:1299–1304.

Warnock, D.E., J.E. Hinshaw, and S.L. Schmid. 1996. Dynamin self-assembly stimulates its GTPase activity. *J. Biol. Chem.* 271:22310–22314.

Yoshida, Y., M. Kinuta, T. Abe, S. Liang, K. Araki, O. Cremona, G. Di Paolo, Y. Moriyama, T. Yasuda, P. De Camilli, and K. Takei. 2004. The stimulatory action of amphiphysin on dynamin function is dependent on lipid bilayer curvature. *EMBO J.*23:3483–3491.